Hindawi
Journal of Nanomaterials
Volume 2019, Article ID 8130419, 11 pages
https://doi.org/10.1155/2019/8130419

Research Article

Nanoclay and Water Uptake Effects on Mechanical Properties of Unsaturated Polyester

Necar Merah and Omer Mohamed

Mechanical Engineering Department, King Fahd University of Petroleum and Minerals, Dhahran 31261, Saudi Arabia

Correspondence should be addressed to Necar Merah; nesar@kfupm.edu.sa

Received 15 September 2018; Accepted 18 November 2018; Published 3 January 2019

Academic Editor: Jim Low

Unsaturated polyester/nanoclay (UP/NC) composites were developed using an optimized process, which combines high shear mixing (HSM) and ultrasonication. Different types of organically modified nanoclays (Cloisites 10A and 20A and Nanomer I.30E) were considered with I.30E resulting in the best morphology with an exfoliated structure. This and the higher aspect ratio of I.30E lead to its better performance under tensile and flexural testing. Different loadings of I.30E (0, 1, 2, 3, and 4 wt%) were thus used to manufacture UP/NC nanocomposites and test their resistance to water uptake as well as the moisture ingress effects on their mechanical properties. The results showed that the addition of I.30E nanoclay enhanced the hydrophobicity of the nanocomposite with a maximum improvement of about 40% at 4 wt% of NC loading. Flexural test results revealed relative degradation in the flexural properties of neat UP and UP/NC, due to moisture uptake. However, the reduction in flexural properties was found to be minimal at the optimum nanoclay loading of 3 wt%.

1. Introduction

Recently, polymer-based nanocomposites are being widely used in industrial applications due to their lightweight, great resistance to chemicals, and excellent insulation properties. These properties give polymers the advantage over metallic and ceramic materials in certain applications: piping, aerospace industry, automobiles, etc. [1–6]. However, polar polymers are well known to have low mechanical properties and low resistance to moisture uptake when compared to other engineering materials. Hence, this challenge attracted the attention of scientists and researchers to enhance the overall performance of polymers by developing polymer-based composites and nanocomposites. The Toyota research group [1, 2] developed a novel nanocomposite by incorporation of nanoclay into poly-6-amide, resulting in improved mechanical properties of the resin. Depending on the processing technique, different microstructures could be formed. The first one is an immiscible structure, in which polymer chains are not penetrating into nanoclay layers and the intercalated structure forms when polymer chains intercalate between reinforcement layers with full penetration while silicate layers' structure is kept in the same order. The last structure is an exfoliated (delaminated) structure wherein silicate layers dispersed fully in polymer resin [1, 2]. Exfoliated structures have been shown to yield optimized physical and mechanical properties [3–6]. Their development depends on the resin and nanoclay types as well as the preparation methods. Bensadoun et al. [3] studied three types of mixing techniques and showed that the mixing method has a significant effect on the morphology of unsaturated polyester-nanoclay composites. The amount of optimum silicate loading that results in the exfoliated structure is highly dependent on the mixing process [5]. Utilizing high shear mixing and ultrasonication led to better dispersion of polymer chains into nanoclay platelets; accordingly, this resulted in improvement in the mechanical properties [5, 6]. Moreover, exposure of polymers to moisture for long periods is seen to degrade their glass transition temperature (T_g) and mechanical properties. The degradation takes place because of water absorption by the resin, which plasticizes the matrix and weakens the bonded area between the matrix and nanosilicate platelets

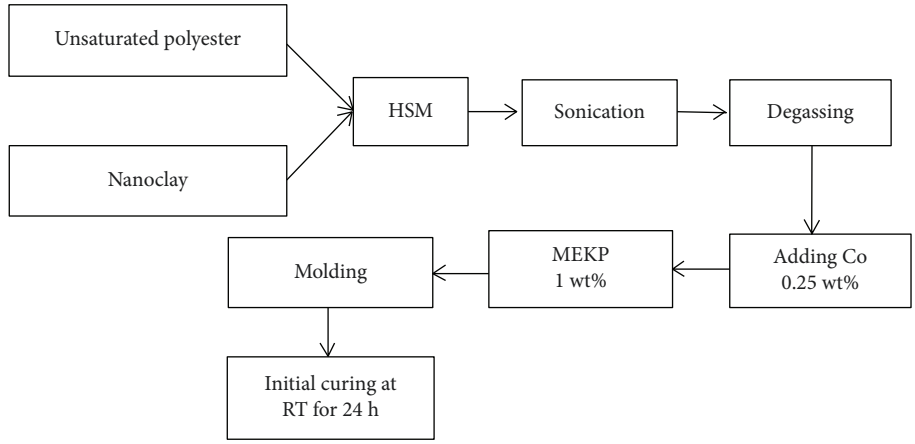

Figure 1: UP/NC fabrication process layout.

[7–9]. Alamri and Low [8] found that the flexural strength and modulus of epoxy-based nanoclay composites decreased due to the water absorption. They however reported that the addition of nanofillers enhanced the flexural strength and modulus of nanocomposites compared to wet unfilled epoxy. Rull et al. [9] concluded that nanoclay reinforcement particles reduced water absorption of glass fiber/unsaturated polyester resin composites and increased its performance in humid environments.

The above review shows that the subject of nanoclay-filled unsaturated polyester has not received sufficient attention from researchers. None of the existing studies has dealt with the effects of nanoclay types on the performance of UP, and a limited work has investigated the combined influence of moisture and clay loading on physical and mechanical properties of UP resin. The present study addresses the effects of different clay types and clay content on the tensile and flexural properties of unsaturated polyester. It investigates the effects of organically modified nanoclay addition on the resistance of UP to water uptake and how both nanoclay loading and moisture affect its physical and flexural properties. Neat UP and UP/NC specimens prepared by optimum mixing and curing processes are immersed in tap water at room temperature for 3 months to investigate the nanocomposite's hydrophobicity and water uptake effects on the flexural properties of the matrix.

2. Experimental Procedure

2.1. Materials. Isophthalic acid-based unsaturated polyester (UP) resin supplied by Gulf Chemicals and Industrial Oils Co. (GCIR), under the commercial name SAUDPOL SP-351-BV13, is used in the study with methyl ethyl ketone peroxide (MEKP) as a hardener. In addition to that, cobalt ethylhexanoate, 6% Co., is added as an accelerator, to increase the curing reaction rate. Different types of montmorillonite clays are utilized, namely, Nanomer I.30E, Cloisite 10A (C10A), and Cloisite 20A (C201A). The choice of these montmorillonite organoclays was based on previous studies carried out on epoxy-clay nanocomposites, which showed that these nanoclays are promising candidates for polymer reinforcement [10]. Nanomer I.30E is modified with primary octadecyl ammonium ion while Cloisite 10A and Cloisite 20A are modified with quaternary dimethyl benzyl hydrogenated tallow ammonium and with quaternary dimethyl dihydrogenated tallow ammonium, respectively. The montmorillonite organoclays have d-spacings ranging from 21 Å for I.30E to 24 Å for C20A. Nanomer I.30E was supplied by Nanocor Inc., USA, while C10A and C20A were acquired from Southern Clay Product, USA.

2.2. Preparation of the UP/NC Nanocomposites. The amount of UP resin to produce a bulk sample ($126 \times 178 \times 4$ mm) was estimated to be 120 g. This quantity of resin was weighed by mass balance and poured into a beaker; then I.30E clay loadings of 1, 2, 3, and 4 wt% were added separately to the resin and mixed manually using a stirring rod for 5 minutes to prevent outpouring of nanoclay (NC) at the beginning of the HSM process. A model L5M-A high shear mixer, manufactured by Silverson, was utilized to disperse NC into the UP resin. Different HSM speeds and mixing periods were considered to optimize the process, resulting in an optimized mixture at a speed of 3000 rpm for 1 hour. A Sonic vc-33 ultrasonicator was then used to remove gaseous bubbles as well as to improve the dispersion of NC into UP [11]. A water bath was utilized, during processing, to keep the viscosity of the mixture constant and to avoid extreme temperatures from being induced into the resin. The final mixture was degassed in a vacuum chamber for 30 minutes to remove any remaining bubbles. After that, the curing agents were added to the mixture before pouring it into the mold. The mold was initially kept under atmospheric conditions for 24 hours to avoid shrinking of polyester. This is followed by optimizing precuring and postcuring processes in a vacuum oven. Figure 1 illustrates the hierarchy of the synthesis process.

As illustrated in Table 1, curing temperatures ranging from 80 to 180°C and curing periods of 2, 3, and 4 hours were considered in the optimization process. After each curing cycle, the glass transition temperature (T_g) was measured to determine the optimized time and temperature.

Table 1: Precuring optimization and postcuring optimization of I.30E.

Temperature optimization		Time optimization	
Precuring temperature (°C)	*Precuring time (h)*	*Precuring temperature (°C)*	*Precuring time (h)*
80			2
120	2	Optimized temperature	3
160			4
Postcuring temperature (°C)	*Postcuring time (h)*	*Postcuring temperature (°C)*	*Postcuring time (h)*
120			2
140	2	Optimized temperature	3
160			4
180			

An earlier work by Mohamed [11] has shown that 3.0 wt% loading of the above described nanoclays resulted in optimum physical and mechanical properties. Thus, Cloisite 10A and Cloisite 20A nanocomposites were prepared using the same procedure but with a clay loading of 3.0 wt% only.

2.3. Thermal and Nanostructural Characterization. The glass transition temperature (T_g) was measured after each curing cycle by METTLER TOLEDO-DSC822e (DSC) according to ASTM D3418-99 standard [12], with a heat rate of 10°C/min and using a thermal cycle in the range of 50–250°C. Bruker D8 Advance X-ray Diffraction (XRD) equipment was used to estimate the degree of intercalation or exfoliation of nanoclay in a polymer matrix, which alters the overall performance of UP/NC nanocomposite. The equipment has a 9-specimen holder with autopositioning feature, and the source of radiation is copper (Cu Kα), with a wavelength of 1.5406 Å. The morphology of the fractured surfaces was examined by FESEM (MERA3, TESCAN).

2.4. Water Uptake Test. Water uptake tests were conducted in accordance with ASTM D570-98 standard [13], but in tap water instead of distilled water. For each condition, three specimens were cut with a computer numerical control (CNC) milling machine to the required dimensions (76.2 mm × 25.4 mm × 4.0 mm). Weight measurements of dry specimens were taken by mass balance before immersing them into tap water at room temperature and atmospheric pressure. After 24 hours of immersion, all specimens were removed from the container, then dried and weighed to determine the weight change. The same procedure was repeated by the end of the first week, then by the end of every two weeks until the specimens approached saturation around 90 days. The weight gain percentage was calculated using

$$M_t = \frac{w_i - w_o}{w_o} \times 100, \quad (1)$$

where M_t is the percentage weight gain after specific immersion time t, w_i is the instantaneous specimen's weight, and w_o is the original specimen's weight, before exposure to water.

2.5. Mechanical Testing. The tensile tests were conducted on a universal testing machine (UTM) according to ASTM D638-02a standard [14]. For each sample, three specimens were machined to a dumbbell-like shape, using the CNC milling machine. The rough surfaces were smoothed by grinding, using carbide abrasive papers. The crosshead motion was adjusted to 1.0 mm/min.

The three-point flexural test was performed in accordance with ASTM-D790-02 standard [15]. Three specimens were cut by the CNC milling machine to the dimensions of 127 mm × 12.7 mm × 4 mm, for each condition. An Instron 3367 testing machine was employed to determine the flexural properties of the specimens. During testing, the span length was adjusted to 60 mm and loading was applied at a rate of 1.15 mm/min.

Three replicas were employed for each of the test conditions, and the average values are reported.

3. Results and Discussions

3.1. Curing of Nanocomposites. Figure 2 shows how the glass transition temperature of I.30E is affected by the precuring temperature and time. Increasing the temperature from 80°C to 120°C, for 2 hours, improved the degree of the cross linking, with T_g increasing by about 12%. However, at 160°C, the glass transition temperature declined to 87°C. This reduction may be due to the degradation of the UP resin, resulting in chain scission. Janković [16] investigated the UP curing process, with MEKP as the initiator, and found that the maximum degree of cure α_{max} varied following a third-order polynomial expression (equation (2)) in the temperature range of 80°C ≤ T ≤ 140°C:

$$\alpha_{max} = 0.87609 - 0.01299 \times T + 1.81102 \times 10^{-4} \times T^2 - 5.88766 \times 10^{-7} \times T^3. \quad (2)$$

Equation (2) predicts that for the present case the maximum degree of cure for the present system is about 0.64 at 80°C and 0.90 at 120°C. This is an indication that crosslinking is almost complete at the latter curing temperature, resulting in the highest T_g. Janković [16] has noted that under isothermal conditions the degree of cure (α) of UP is less than 1.0, due to the presence of an unreacted monomer in the resin.

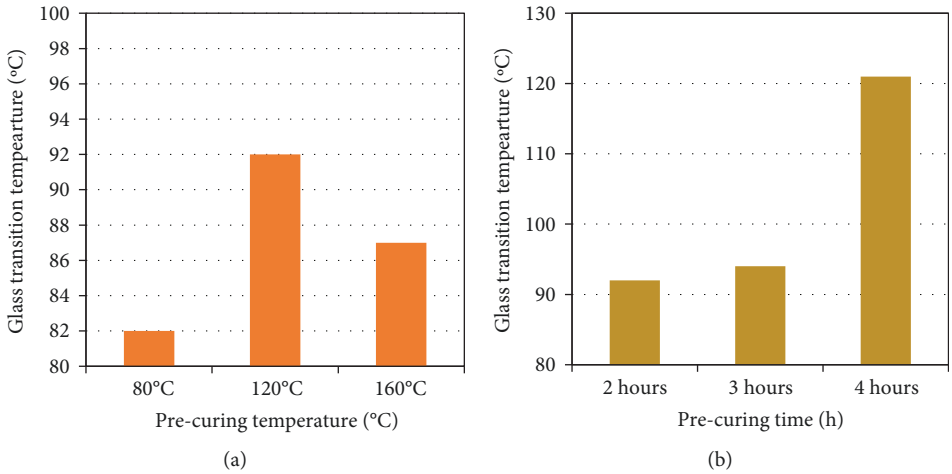

Figure 2: Variation of glass transition temperature of 3 wt% nanoclay with (a) precuring time for 2 h and (b) precuring temperature at 120°C.

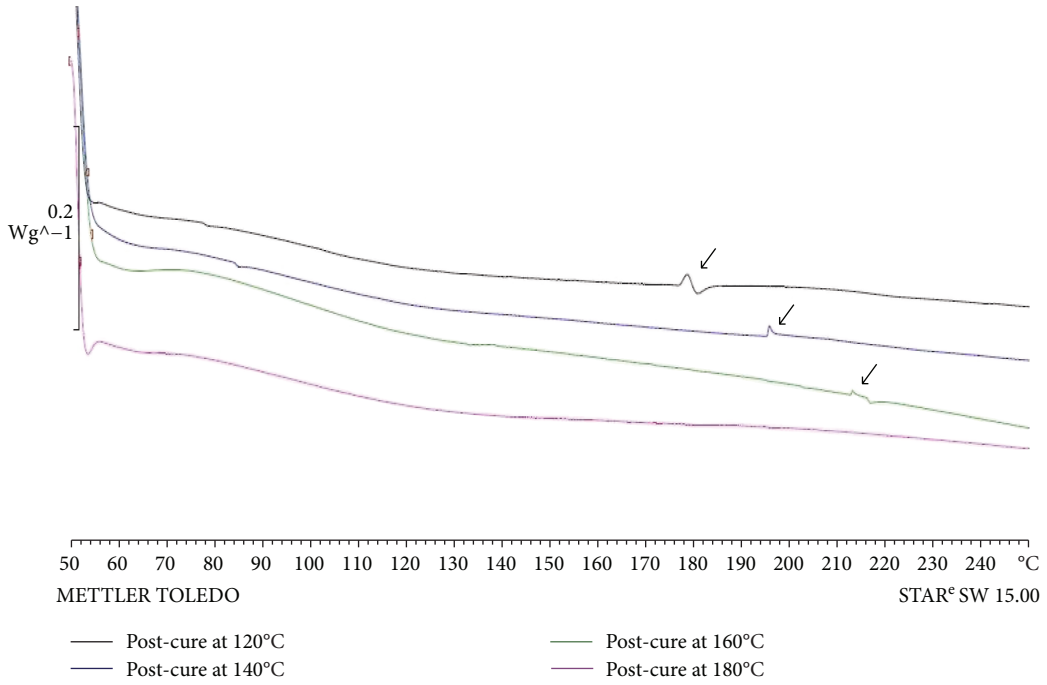

Figure 3: DSC thermograms of postcured specimen, prepared with 3.0 wt% of I.30E NC, at different curing temperatures while curing time fixed at 2 hours.

Figure 2(b) shows that increasing curing time, under 120°C, from 2 hours to 3 hours has a slight effect on glass transition temperature while an additional curing hour resulted in a noticeable increase in T_g. The precuring stage was followed by postcuring (Table 1) in order to examine how additional curing affects T_g of UP/NC composite. It was observed that with additional curing, UP showed some degree of crystallinity, which was proven by the presence of exothermic and endothermic peaks on the DSC thermograms (Figure 3). Meanwhile, rising of postcuring temperature above 120°C showed a shift in exothermic and endothermic peaks to the right while the peak size decreased subsequently until they disappeared above 160°C. The results showed that postcuring for 2 hours at 120°C yielded a T_g of about 178°C. Higher postcuring temperatures and times confirmed the decomposition of the UP, represented by the absence of exothermic and endothermic peaks in the thermograms and by the observed specimen change of color to brown. Similar results were reported by With et al. [17].

3.2. Effect of NC Type on the Morphology of UP/NC Nanocomposites. As mentioned above, three different types of nanoclays (Nanomer I.30E, Cloisite 10A, and Cloisite 20A) were chosen to study the effect of clay type on the

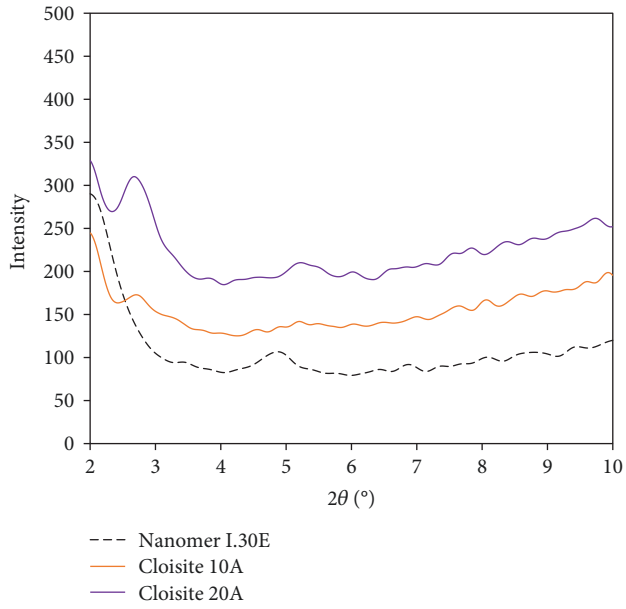

Figure 4: XRD spectra for UP/NC nanocomposites containing 3 wt% of different nanoclay types.

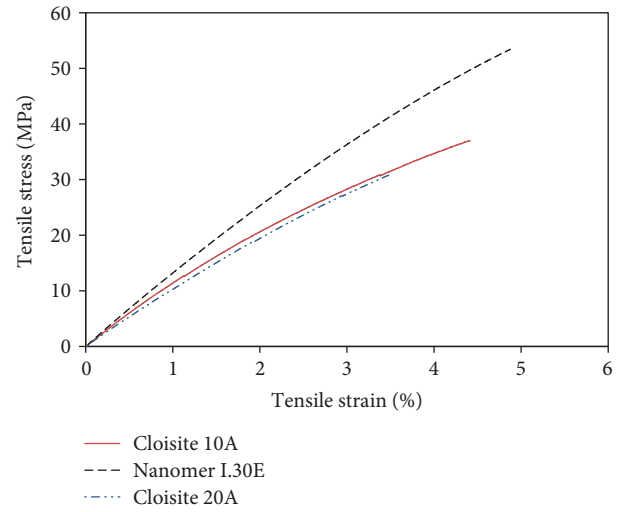

Figure 5: Typical stress-strain curves for UP/NC prepared from the different clay types (3.0 wt%).

morphology and flexural properties of the nanocomposite. To study the morphology of UP/NC, XRD, which is the most common characterization technique used to examine and identify a nanocomposite structure, was chosen. Figure 4 represents the XRD spectra for UP/NC nanocomposites fabricated with the three different clay types. These nanocomposites were prepared with a clay content of 3.0 wt%, using the optimum parameters mentioned above. It is clear that Cloisite nanoclays show diffraction peaks at a Bragg angle of 2.74°, while Nanomer I.30E has no peaks between 2 and 4°. By knowing the diffraction angle at the peak, interlayer spacing could be estimated using Bragg's law (equation (3)).

$$n\lambda = 2d \sin\theta, \tag{3}$$

where n is an integer constant, considered to be 1 in case of principal reflection, λ is the wavelength of incident X-ray, θ is the scattering angle, and d is the planar or interlayer spacing.

Thus, d-spacing for Cloisites was estimated to be 3.2 nm, making the resulting structure an intercalated one [18]. The absence of peaks, at Bragg angles between 2 and 4°, for I.30E, is an indication of an exfoliated/disorder-intercalated structure. Furthermore, UP/NC prepared with I.30E shows a broadened peak at about 4.8°, which is close to the nanoclay diffraction angle of 4.22° [11]. This is another indication that mechanical exfoliation may have been achieved for I.30E nanocomposite [18]. In addition and as reported by Laske et al. [19], the smaller area under the curve means better exfoliation due to the low probability of X-rays to hit the particles. Based on the above discussion, UP/NC nanocomposite prepared by I.30E nanoclay is considered to reveal a good dispersion state and thus is expected to result in a nanocomposite with better physical and mechanical properties as will be shown in the next section.

3.3. Effect of Nanoclay Type and Content on Tensile Properties of UP/NC. The typical stress-strain curves for nanocomposites prepared from different clay types (Nanomer I.30E, Cloisite 10A, and Cloisite 20A) are shown in Figure 5. All nancomposites were synthesized with 3.0 wt% clay loading, using the abovementioned optimized parameters. The loading of 3.0 wt% was selected as it resulted in the optimum improvement in mechanical properties [11]. It is clear that the nanocomposite containing I.30E outperforms both Cloisites in stiffness, strength, and fracture strain. All specimens were fractured in semibrittle mode with no plastic deformation.

The average values of tensile strengths, fracture strains, and modulus of elasticity, for the 3 types of nanoclays, are compared in Figures 6(a)–6(c), respectively. Among the three types of nanocomposites, the one prepared with Nanomer I.30E shows the highest average tensile strength (52.6 MPa), average strain at fracture (5%), and modulus of elasticity (13.7 GPa). The improvement in tensile strength is about 75% over that of pristine UP. The strengths of Cloisite 10A and Cloisite 20A are, respectively, 10% and 24% higher than that of UP. Similar conclusions can be drawn for fracture strain and stiffness. Al-Qadhi and Merah [10] prepared epoxy/nanoclay nanocomposites using C10A, C20A, I.28E, and I.30E, concluding that the latter yielded the highest tensile properties compared to the others. The enhancements in the tensile properties are due to the high aspect ratio of I.30E nanoclay and to better dispersion of the monomer in the resin as is evident from the results in Figure 4. In addition, Cloisites are modified with quaternary dimethyl dihydrogenated tallow ammonium, which is a larger organic modifier as compared to primary octadecyl ammonium. Furthermore, a certain amount of styrene molecules may have been absorbed by nanoclay platelets during mixing and sonication causing a change in crosslink density. In addition to the

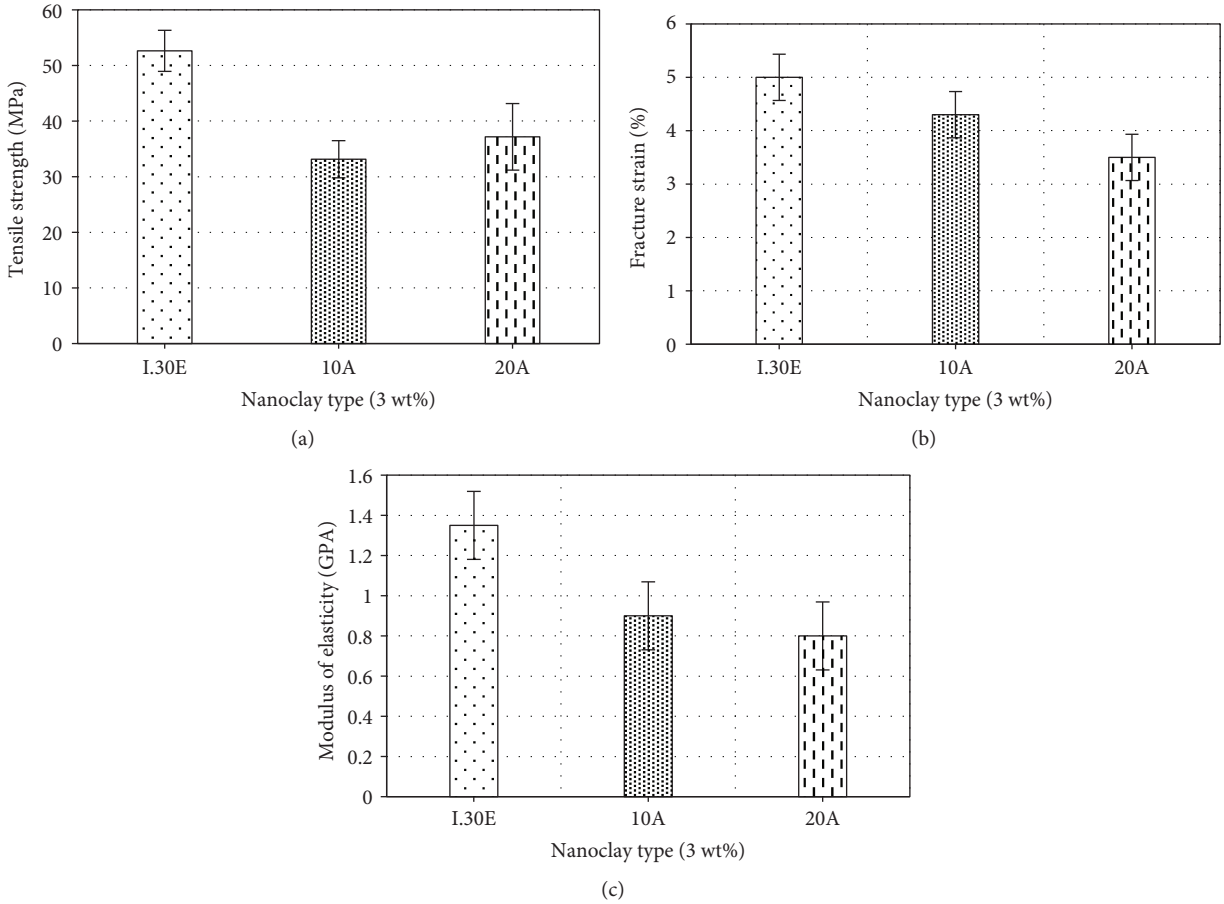

Figure 6: The effect of nanoclay type on (a) the tensile strength, (b) fracture strain, and (c) modulus of elasticity of UP/NC nanocomposites.

mixing techniques and the size of organic modifier, the improvement in the nanocomposites is also affected by the compatibility between the organic modifier and the monomer [20]. Because of its better performance, Nanoclay I.30E is thus chosen to study the effects of clay loading on moisture barrier and mechanical properties of UP/NC.

The effect of I.30E nanoclay loadings on the average tensile properties of the nanocomposite is illustrated in Figure 7. It is clear that as clay loading increases, the tensile strength (Figure 8(a)) and fracture strain of the nanocomposite increase. Both properties reach their maximum value at 3 wt% of clay loading. This corresponds to 75% and 67% improvements in the tensile strength and fracture strain, respectively.

The enhancement in these properties is mainly due to the good dispersion of clay platelets and adherence between clays and UP chains, leading to the improvement of load transfer mechanism between the matrix and nanoclays. However, going beyond 3 wt% decreased both tensile strength and fracture strain. This is because, at higher clay loading, the probability of clay particle agglomeration becomes higher, and hence, these clay clusters create stress raisers that decrease the tensile strength. Al-Qadhi et al. [21] and Rafiq and Merah [7] have observed clay clusters and microvoids, for high clay loadings, at which cracks have initiated. Clay agglomeration and air bubbles happen because of the increase in the viscosity of the mixture at high clay loadings making the formation of exfoliated/disorder intercalated structure a difficult task due to inadequate diffusion of polyester chains between the nanoclay platelets. The enhancement trend observed for strength and toughness is not followed by the material's stiffness (Figure 8(c)); the modulus of elasticity decreased slightly with the addition of 1.0 wt% NC, before recovering its initial value at 3.0 wt% loading. Taking into consideration the large

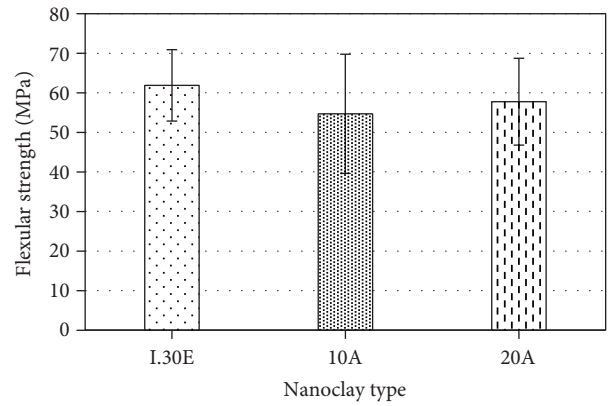

Figure 7: The effect of clay type on the flexural strength of the UP/NC containing 3.0 wt% of I.30E NC.

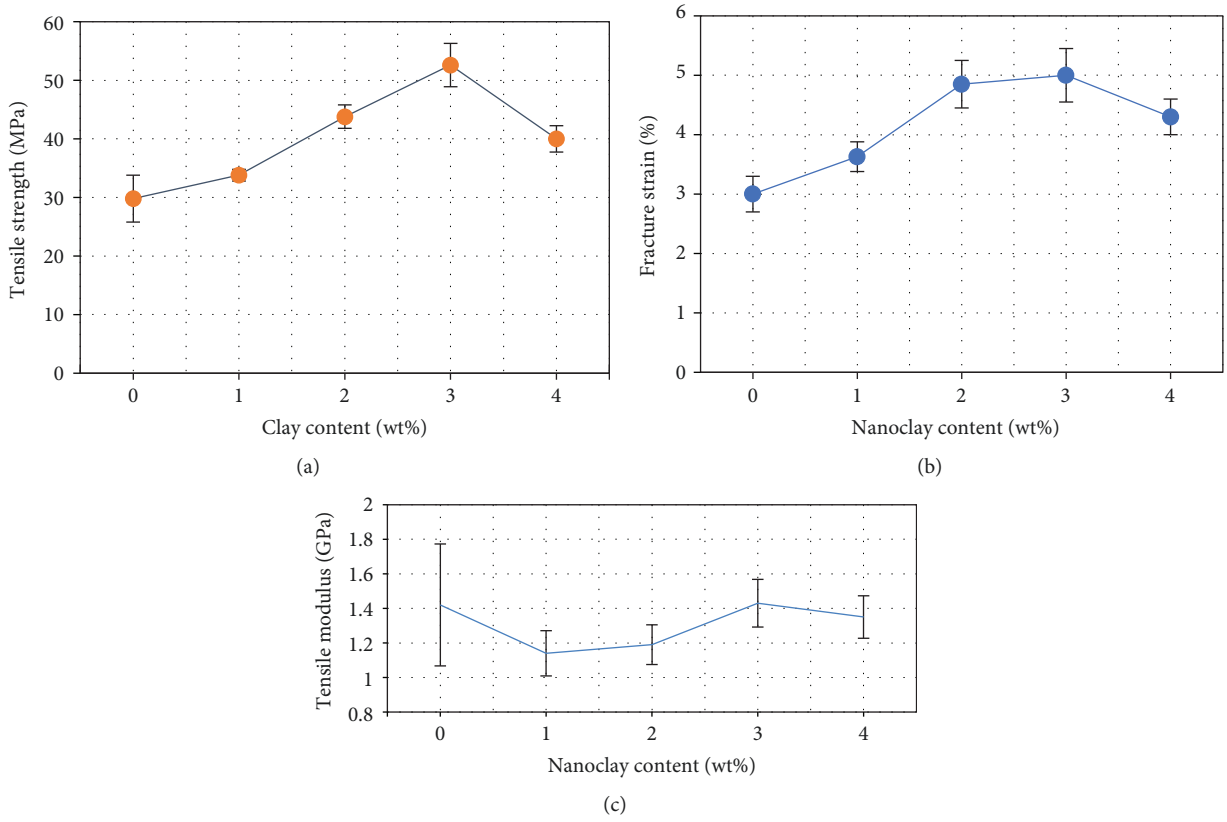

FIGURE 8: The effect of I.30E clay loading on (a) the tensile strength, (b) fracture strain, and (c) tensile modulus of UP/NC nanocomposites.

margin of error associated with the determination of the modulus, it can be concluded that the clay content has little or no effect on the stiffness of the developed UP. This behavior is similar to what has been reported by Bensadoun et al. [3] for unsaturated polyester resin.

3.4. Effect of Clay Type and Loading on Flexural Properties of UP/NC. Figure 7 shows a comparison of average flexural strengths for the nanocomposites prepared with 3.0 wt% of I.30E, C10A, and C20A. Similar to what was observed for tensile strength, it is clear that the nanocomposites prepared with Nanomer I.30E performed better than those prepared with Cloisites in terms of flexural strength. The improvement over pristine UP is about 56%. Furthermore, the difference between the strengths of the composites prepared by the Nanomer and those synthesized with the Cloisites is smaller than that seen for tensile strength.

The results of Figure 9(a) show that the improvement in flexural strength with I.30E clay content is almost linear, reaching its maximum value of 62 MPa (56% increase over pristine UP) at 3 wt%. As mentioned above, the positive effect of clay on the strength is attributable to good dispersion of clay in UP and excellent adhesion of resin to clay platelets, while the degradation at 4 wt% can be attributed to the presence of clay agglomerations and/or voids, forming stress raisers that tend to weaken UP/NC composite.

The effect of clay loading on the flexural modulus (Figure 9(a)) is similar to that observed for tensile modulus and what has been reported by Kchit et al. [22]. Other researchers have found that clay loading increased the stiffness of polymers [4, 21, 22], usually at clay contents higher than 4%.

The effects of clay addition on the fractured surfaces' morphology for pristine UP and UP/NC nanocomposites (1.0, 3.0, and 4.0 wt%) are illustrated in Figure 10. These fractographs reveal that the morphology of the fractured surfaces becomes coarser as clay loading increases. The rough fractured surfaces of Figures 10(b)–10(d) are probably due to the changing in crack directions because of the presence of nanoclay platelets or clusters ahead of crack paths promoting the formation of a number of microcracks (indicated by the arrows). The presence of long secondary cracks (Figure 10(d)) could be due to stress concentration caused by clay clustering at 4.0 wt%, which compromises the advantage of nanoclay's aspect ratio and leads to the observed lower strengths and fracture strains for this clay content.

3.5. Effect of Clay Loading on the Water Uptake of UP. The variation of the difference in weight gain percentage (W_t) with square root of immersion time (hours) for UP and UP/NC nanocomposites is plotted in Figure 11, showing that the variation of W_t with $\sqrt{t}$ follows a linear trend during the first 8 immersion days (14 hours$^{0.5}$), indicating that all specimens are undergoing diffusion-controlled behavior. The diffusion phase is followed by a surge in water uptake rate up to 21 days of immersion. The third phase is characterized by lower uptake rate leading to the beginning of saturation after 78 days. The highest maximum water absorption

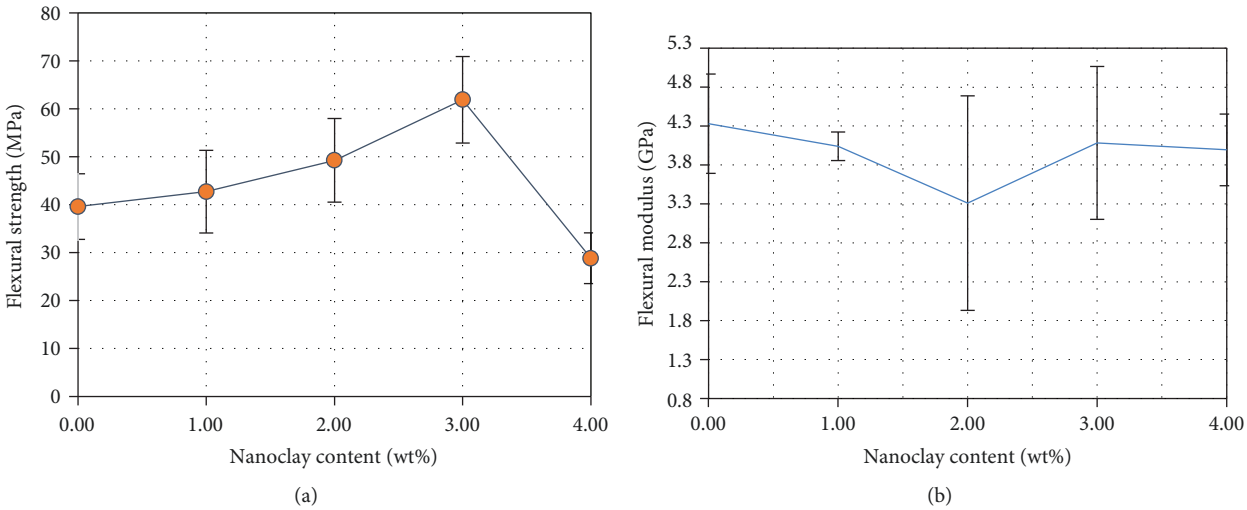

Figure 9: The effect of clay loading on the flexural strength of the UP/NC prepared with I.30E NC.

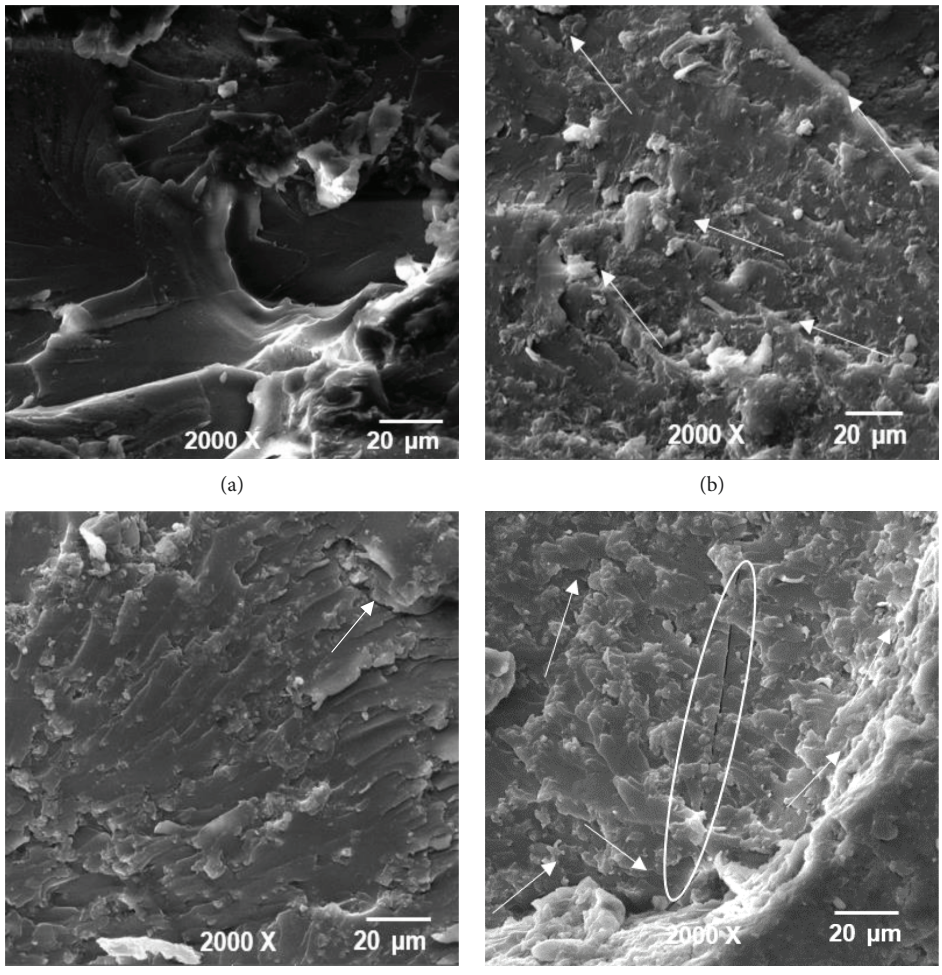

Figure 10: SEM fractographs of UP and UP/NC with (a) 0 wt%, (b) 1 wt%, (c) 3 wt%, and (d) 4 wt% I.30E clay loadings.

was found to be above 1.6% for neat UP. This material is known to contain hydrophilic functional groups, such as hydroxyl and amino-methyl which have affinity to water [23]. The addition of nanoclay leads to a noticeable decrease in maximum water uptake. As can be seen in Figure 12, the water weight gain decreases linearly with clay content. The

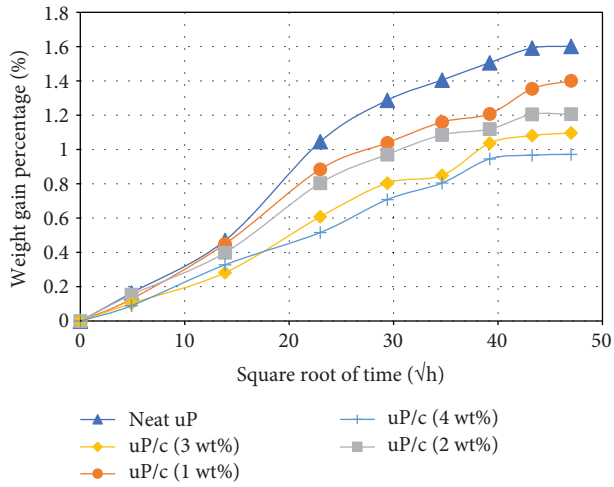

Figure 11: Variation of moisture weight gain percentage with square root of immersion time (hours$^{0.5}$) for neat UP and UP/NC containing 1, 2, 3, and 4 wt% of I.30E NC.

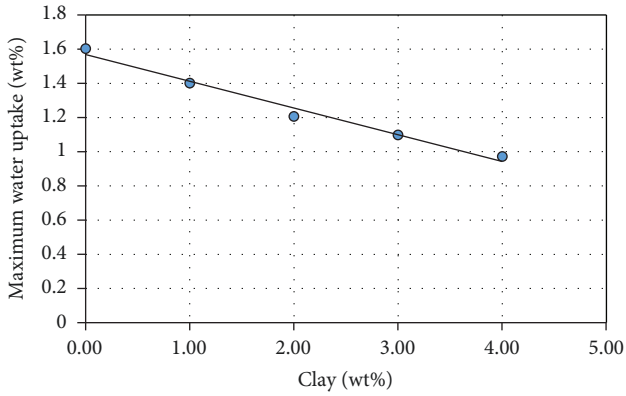

Figure 12: Variation of maximum water uptake with I.30E clay content.

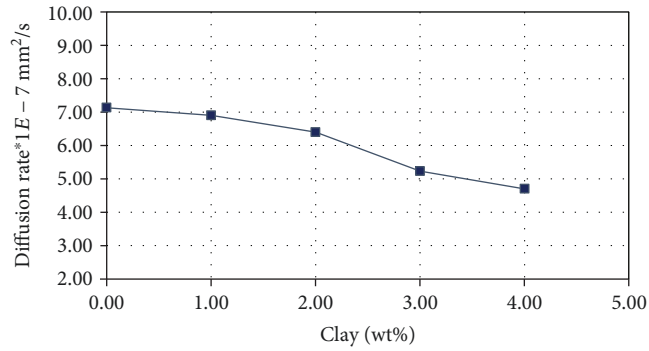

Figure 13: The effect of I.30E NC loading on the diffusion coefficient for UP.

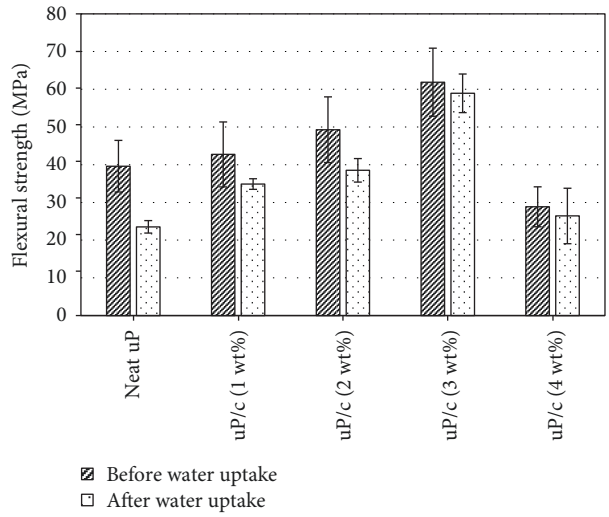

Figure 14: The effect of water uptake on the flexural strength of neat UP and UP/NC (I.30E) nanocomposites for both dry and wet specimens.

improvement in water uptake resistance is mainly attributed to the high aspect ratio of nanoclay, which creates tortious paths for the water molecules [6–9, 21].

As mentioned above, the linear trend of weight gain percentage over square root of time, during the first few days of immersion, was an indication that the water uptake behavior is diffusion controlled. For this reason, Fick's law was used to describe the diffusivity of UP and UP/NC nanocomposites. Assuming that all materials are homogenous and the diffusion is a one-dimensional process through the specimen's thickness (h), Fick's law (equation 3) could be used to describe the present water uptake behavior [24].

$$M_t = \frac{4M_S}{h}\sqrt{t/\pi} \times \sqrt{D}, \tag{3}$$

where M_t is the water gain percentage at time t (seconds), M_s is the water gain percentage at the saturation, D is the diffusion coefficient (mm^2/s), and h is the specimen's thickness.

Figure 13 illustrates the effect of NC loading on the diffusion coefficient estimated from experimental results, using equation (3), for UP and UP/c nanocomposites. The diffusion coefficient seems to be less sensitive to clay loading up to 2.0 wt% and sharply decreases thereafter with clay loading. The lower diffusion rate UP/NC is due to the presence of nanoclay platelets, which act as impermeable barriers to the diffusing molecules. The lower diffusion rate for nanocomposites has contributed to the reduction in the maximum water uptake reported in Figure 12. It should be mentioned that it is very difficult to accurately measure the difference in weight at low values of water uptake.

3.6. Combined Effect of Clay Content and Water Uptake on Flexural Strength. Figure 14 shows that water uptake has a considerable negative influence of the flexural strength of neat unsaturated polyester. The flexural strength decreased by 40% due to 1.6% of total water uptake; moisture is known to act as a plasticizer for polymers in general. The effect of nanoclay addition in improving the resistance

to plasticization is evident from the difference in the height of the bars representing the flexural strength of UP/NC; introducing only 1 and 2 wt% of NC resulted in lowering the degradation effect of water uptake by more than 50%, while the reduction in the flexural strength was found to be less than 10% in the case of UP/NC nanocomposites prepared with higher clay loading (3 and 4 wt%). This is confirming that nanoclay enhanced the barrier properties of the developed nanocomposites [21].

4. Conclusions

The present investigation showed that among the three types of nanoclay: C10A, C20A, and I.30E, considered in the analysis, the latter resulted in better dispersion in unsaturated polyester and thus lead to better performance of UP/NC. Tensile and flexural strengths of nanocomposites prepared with I.30E increased linearly with clay content, reaching a maximum at 3.0 wt% loading. This optimum clay addition resulted in 75% and 56% improvements in tensile and flexural strengths, respectively. Possible clay agglomerations have resulted in the degradation of the nanocomposite's strength at higher clay content. The material's fracture strain followed the same trend as the strength. Clay loading has an insignificant effect on the resin's stiffnesses.

The maximum water uptake was found to vary linearly with clay content, decreasing substantially with increasing clay loading. The water barrier property of I.30E nanoclay has minimized the plasticization effect of the moisture and thus reduced the polymer's flexural strength degradation. This degradation varied from 40% for neat UP to only 10% for UP/NC with I.30E clay loading of 3.0 wt%, which has resulted in the highest strength.

Data Availability

Previously reported experimental data were used to support this study and are available in MSc thesis cited in the text as a reference [10].

Conflicts of Interest

The authors declare that they have no conflicts of interest.

Acknowledgments

The authors of this work acknowledged King Fahd University of Petroleum and Minerals (KFUPM) for their support and thanked Gulf Chemicals and Industrial Oils Co. (GCIR) for providing the unsaturated polyester besides the curing agents.

References

[1] D. R. Paul and L. M. Robeson, "Polymer nanotechnology: nanocomposites," *Polymer*, vol. 49, no. 15, pp. 3187–3204, 2008.

[2] P. J. Schubel, M. S. Johnson, N. A. Warrior, and C. D. Rudd, "Characterisation of thermoset laminates for cosmetic automotive applications: Part III – Shrinkage control via nanoscale reinforcement," *Composites Part A: Applied Science and Manufacturing*, vol. 37, no. 10, pp. 1757–1772, 2006.

[3] F. Bensadoun, N. Kchit, C. Billotte, F. Trochu, and E. Ruiz, "A comparative study of dispersion techniques for nanocomposite made with nanoclays and an unsaturated polyester resin," *Journal of Nanomaterials*, vol. 2011, 12 pages, 2011.

[4] N. Merah and M. Al-Qadhi, "Effects of processing techniques on morphology and mechanical properties of epoxy-clay nanocomposites," *Advances in Materials Research*, vol. 652-654, pp. 167–174, 2013.

[5] B. C. Kim, S. W. Park, and D. G. Lee, "Fracture toughness of the nano-particle reinforced epoxy composite," *Composite Structures*, vol. 86, no. 1–3, pp. 69–77, 2008.

[6] O. Zabihi, M. Ahmadi, S. Nikafshar, K. C. Preyeswary, and M. Naeb, "A technical review on epoxy-clay nanocomposites: structure, properties, and their applications in fiber reinforced composites," *Composites Part B: Engineering*, vol. 135, pp. 1–24, 2018.

[7] A. Rafiq and N. Merah, "Nanoclay enhancement of flexural properties and water uptake resistance of GFR epoxy composites at different temperatures," *Journal of Composite Materials*, 2018.

[8] H. Alamri and I. M. Low, "Effect of water absorption on the mechanical properties of nanoclay filled recycled cellulose fibre reinforced epoxy hybrid nanocomposites," *Composites Part A, Applied Science and Manufacturing*, vol. 44, no. 1, pp. 23–31, 2013.

[9] N. Rull, R. P. Ollier, G. Francucci, E. S. Rodriguez, and V. A. Alvarez, "Effect of the addition of nanoclays on the water absorption and mechanical properties of glass fiber/up resin composites," *Journal of Composite Materials*, vol. 49, no. 13, pp. 1629–1637, 2015.

[10] M. Al-Qadhi and N. Merah, "Mechanical and physical properties of polymer-based nanocomposites containing different types of clay," *Polymer Composites*, vol. 36, no. 11, pp. 1998–2007, 2015.

[11] O. M. A. Mohamed, *Development and Characterization of Hybrid Glass Fiber Reinforced Unsaturated Polyester/Clay Nanocomposite, [M.S. thesis]*, KFUPM, 2017.

[12] S. Calorimetry, "Standard test Method for Transition Temperatures of Polymer By Differential," *Test*, vol. 8, pp. 1–7, 2004.

[13] Annual Book of ASTM Standards, D570-98 (Reapproved 2005), *Standard test method for water absorption of plastics*, ASTM International, West Conshohocken, PA, USA, 2015.

[14] *Annual Book of ASTM Standards D638*, ASTM International, West Conshohocken, PA, USA, 2013.

[15] Annual Book of ASTM Standards, D 790-02, *Standard Test Methods for Flexural Properties of Unreinforced and Reinforced Plastics and Electrical Insulating Materials*, ASTM International, West Conshohocken, PA, USA, 2002.

[16] B. Janković, "The kinetic analysis of isothermal curing reaction of an unsaturated polyester resin: estimation of the density distribution function of the apparent activation energy," *Chemical Engineering Journal*, vol. 162, no. 1, pp. 331–340, 2010.

[17] P. With, P. Amic, and R. J. Farris, "Thermal and mechanical properties of the precursor polymers: comparison of their properties with poly(amic acid)," *Polymer Engineering and Science*, vol. 39, no. 4, pp. 638–645, 1999.

[18] L. A. Utracki, *Clay-Containing Polymeric Nanocomposites, Volumes 1-2, First Edition*, ismithers rapra, 2004.

[19] H. M. Stephan Laske, I. Duretek, and A. Witschnigg, "Influence of the degree of exfoliation on the thermal conductivity of polypropylene nanocomposites," *Polymer Engineering & Science*, vol. 52, no. 8, pp. 1749–1753, 2012.

[20] S. Gârea, H. Iovu, and G. Voicu, "The influence of some new montmorillonite modifier agents on the epoxy–montmorillonite nanocomposites structure," *Applied Clay Science*, vol. 50, no. 4, pp. 469–475, 2010.

[21] M. Al-Qadhi, N. Merah, Z. M. Gasem, N. Abu-Dheir, and B. J. Aleem, "Effect of water and crude oil on mechanical and thermal properties of epoxy-clay nanocomposites," *Polymer Composites*, vol. 35, no. 2, pp. 318–326, 2014.

[22] N. Kchit, F. Bensadoun, T. Carrozani, C. Billotte, E. Ruiz, and F. Trochu, "A study of nanoclay composites fabricated by liquid composite," in *The 10th International Conference on Flow Processes in Composite Materials (FPCM10)*, Monte Verità, Ascona, 2010.

[23] N. Ogata, K. Sanui, Y. Shimozato, and S. Munemura, "Syntheses of functional condensation polymer. I. Polyesters having pendant functional groups such as hydroxyl, formyl, aldoxime, aminomethyl and hydroxymethyl," *Journal of Polymer Science: Polymer Chemistry Edition*, vol. 14, no. 12, pp. 2969–2981, 1976.

[24] H. N. Dhakal, Z. Y. Zhang, and M. O. W. Richardson, "Effect of water absorption on the mechanical properties of hemp fibre reinforced unsaturated polyester composites," *Composites Science and Technology*, vol. 67, no. 7-8, pp. 1674–1683, 2007.

[25] R. Ollier, E. Rodriguez, and V. Alvarez, "Unsaturated polyester/bentonite nanocomposites: influence of clay modification on final performance," *Composites Part A: Applied Science and Manufacturing*, vol. 48, pp. 137–143, 2013.